SYNTHESIS BY SOL-GEL AND CYTOTOXICITY OF ZINC OXIDE NANOPARTICLES USING WASTED ALKALINE BATTERIES

C. L. DÍAZ DE LEÓN[a], I. OLIVAS-ARMENDARIZ[a], J.F. HERNÁNDEZ PAZ[a], C. D. GÓMEZ-ESPARZA[a], H. REYES-BLAS[a], M. HERNÁNDEZ GONZÁLEZ[b], C. VELASCO-SANTOS[c], J.L RIVERA-ARMENTA[d], C. A. RODRÍGUEZ-GONZÁLEZ[a*]

[a]*Technology and Engineering Institute, Autonomous University of Juarez City, Av. del Charro #610 norte, Col. Partido Romero, C.P. 32320, Ciudad Juárez, Chihuahua, México.*

[b]*Agrarian Autonomous University, Antonio Narro, Calzada Antonio Narro 1923, Buenavista, Saltillo Coahuila, 25315, México.*

[c]*Division of Postgraduate Studies and Research, Technological Institute of Queretaro, Av. Tecnológico S/N, Col. Centro Histórico, C.P. 76000, Santiago de Querétaro, Querétaro, México.*

[d]*Center for Research in Secondary Petrochemicals. Technological Institute of Ciudad Madero, Prol. Bahia de Aldahir y Ave. De las bahías, s/n Parque de la pequeña y mediana industria, Altamira, Tamaulipas, Mexico.*

High purity hexagonal Zinc Oxide nanoparticles were synthesized by sol gel method using wasted anodes of alkaline batteries as raw material. Zinc leaching was carried out using nitric acid. Atomic absorption, Field Emission Gun Scanning Electron Microscopy, Energy Dispersive X-Ray Analysis, X-Ray Fluorescence, X-Ray Diffraction, Transmission Electron Microscopy and Dynamic Light Scattering were used to characterize process powders and the obtained NPs. Starch and dextrose were proven as suitable sol gel agents. Nanoparticle sizes in the range of 20 to 160 nm were obtained depending on calcination temperatures. According the percentage of viability obtained by the ISO 10993-5:2009(E) assays the ZnO NPs in concentrations from 1 to 7% showed a cytotoxic effect when exposed to 3T3 fibroblasts cells.

(Received October 28, 2016; Accepted May 6, 2017)

Keywords: Zinc oxide nanopoarticles, Sol gel method, Wasted batteries

1. Introduction

Zinc Oxide (ZnO) is a widely used non-toxic multifunctional material. It exhibits high chemical, thermal and mechanical stability, high photostability, piezoelectricity and biocompatibility among other properties [1,2]. The ZnO crystal structure is hexagonal at room temperature, its space group and lattice constants are c6mc, a = 0.3296 and c = 0.520 nm [3,4].

Zinc oxide nanostructures are commonly used as fillers in polymeric materials for the pharmaceutical and cosmetic industry, as UV-absorbers, coatings and packaging. Improvements in mechanical properties, wetting angle, UV protection and antimicrobial properties are reported in nanocomposites when ZnO is used, even in small amounts (1%) [6-11].

Currently, many ZnO nanostructures have been synthetized for several routes such as vapor deposition, hydrothermal processes, precipitation, micro-emulsion, mechano-chemical processes, sonochemical routes and sol gel. These methods allow obtaining ZnO nanostructures in numerous shapes and sizes including nanowires, needles, springs, rings, tubes, belts and flowers. [12-24]. Despite the many publications on the synthesis of ZnO NPs, there is still great interest to

[*]Corresponding author: claudia.rodriguez@uacj.mx

narrow particle size distribution using less contaminant reactants, more environmental friendly processes and reducing costs.

In the case of wet chemistry methods to obtain ZnO nanoparticles such as sol-gel, several authors have reported the effect of polymerizing agents to control their shape and size. Among these agents are polietilenglycol, oleic acid, gelatin and starch [25-30]. Starch has a good chemical stability compared with other carbohydrates due to the hydroxyl group reactivity of the a-glucose units. These hydroxyl groups can react in a similar manner that primary and secondary alcohols do, therefore they can be used as sol-gel agents to produce ZnO nanoparticles as reported by H. Staroszczyk et al and Zhang et al in 2010 and 2011[28,29]. Khorsand Zak et. al in 2012 [30] also reported the synthesis of ZnO nanoparticles with a narrow particle size distribution using starch as sol-gel agent. Dextrose is an isomer of glucose which has high water solubility and low cost [31] and it has also been used in sol-gel processes, mainly as a reducing agent, to obtain nanoparticles [32].

In recent years some researchers have reported the cytotoxic effect of ZnO nanoparticles [33-36]. The results showed that the toxicity mechanism of the ZnO nanoparticles depends of factors like size, concentration, morphology, and surface modification [37]. Results showed that the cytotoxic effects were higher when concentration was increased and particle size decreased [38]. Small particles exhibit large interfacial area and penetrates the cell´s membrane more easily [39] and at higher concentrations poor cellular uptake are obtained, resulting in higher cell death [37, 38, 40].However, other researchers have not found a relationship between cytotoxic effect and particle size [41]. Some studies found that cytotoxic effect is also affected by the morphology of ZnO nanoparticles [38, 42]. It is reported that nanorods and nanowires shape penetrates more easily the membrane cell than nanoparticle with spherical shape. This could be attributed to the higher amount of oxygen vacancies of the polar facets of the ZnO nanorods and nanowires that results in damage to cell´s DNA, proteins and membranes due to the oxidative stress and inflammation [34].

Regarding the cost reduction of ZnO nanoparticles, in 2011 Berger [43] et al reported the economic feasibility of ZnO NPs production of 40 to 50 nm using the complete electrode of waste alkaline batteries (that includes Zn and Mn powders) as raw material. They used HCl, Hexane and Cyanex 923 solutions for the Zn leaching and ZnO NPs production. The aim of this work is to obtain ZnO NPs from anodes of waste alkaline batteries, leach with nitric acid to obtain zinc nitrate that allows the use of non-toxic abundant sol gel agents such as starch or dextrose, characterize them and determine their cytotoxicity.

2. Experimental procedure

Waste alkaline type D batteries were used as zinc source for the NPs synthesis. Batteries were cut longitudinally and their anodes were manually separated from the rest of the materials, weighed and analyzed by atomic absorption to quantify the Zinc content. Then, they were pulverized using an agate mortar and washed three times with deionized water to remove contaminants. Scanning electron microscopy (Jeol JSM-7000F), Energy Dispersive X-Ray spectroscopy (EDAX) X-Ray Diffraction (XRD, X'Pert Pro PANalytical, λ=0.1542 nm), and X-Ray Fluorescence (Thermo Scientific ARL) analysis were performed before and after the washing process. Subsequently, the washed powders were leached using nitric acid (HNO_3 JTBaker 9621-02) and hydrogen oxygen peroxide (H_2O_2, Jaloma S.A.) in the following proportion: Zn-HNO_3-H_2O_2. Reactions at equilibrium were calculated using the FACTSage@ Equilibrium program. Once the leached solution was obtained, the ZnO Nps were synthesized by sol-gel methods using starch and dextrose as sol-gel agents. In the case where starch was used, 10 g of rice starch (Sigma-Aldrich S7260) were dissolved in 150 ml of deionized water at 75^{o}C during 30 min. Then, the leached solution was added and the agitation was maintained during 10h at 80^{o}C. Afterwards, the material was dried in an oven during 24 h at 100^{o}C. Thermo-gravimetric analysis (TA Instrument-SDT2960) was performed on the dried gels to determine the calcination temperature. Calcination was done in a temperature range from 400^{o}C to 800^{o}C. When dextrose was used as sol gel agent, 21.4g of dextrose (JT Baker DGlucose 1916-01) were mixed with 150 ml of deionized

water and the procedure described above for starch was followed except that agitation time was 5h instead of 10h. The resulting NPs were characterized by the techniques previously mentioned, as well as Transmission Electron Microscopy (Jeol JEM-2200FS) and Dynamic Light Scattering (Mictotrac-Nanotrac Wave Zetrator).

The cytotoxicity assay was performed using 3T3 fibroblasts cells which were seeded in sterilized nanoparticles (Synthetized using starch and calcined at 400oC) in a 96 well culture plate and maintained in DMEM supplemented with 10% FBS and 1% streptomycin/penicillin at 37°C humidified with 5% CO_2. Cells cultured in a blank well were used as a control. After 24 and 72 hours, the medium was discarded and replaced with new medium containing MTT (0.5 mg/mL) and incubated for 3 h at 37 °C. The resulting crystals formazan were dissolved in dimethyl sulfoxide and the absorbance of the solutions were read at 570 nm (Benchmark Plus, microplate 152 spectrophotometer BioRad).

3. Results and discussion

After disassembling the waste alkaline batteries it was found that the anodes' weight is approximately the 25% of the total weight of the batteries. This is in agreement with previous reports [43]. According to the atomic absorption analysis the Zinc content on waste anodes varies from 66 to 68%. Fig. 1 a, b, c and d show an example of the SEM and EDS analysis of the powder from the anodes of waste batteries before and after the washing process described in the experimental procedure. The waste anodes contain heterogeneous particles with sizes in the range between 40 nm to 6 μm. These particles are made of Zinc (Zn), Oxygen (O), Potassium (K) and Carbon (C). Carbon could also come from the SEM sample preparation process and Potassium comes from the alkaline electrolytes used in the batteries which are typically made of potassium hydroxide (KOH) [44, 45]. According to the EDS analysis, Potassium can be removed during the washing process due to its water solubility.

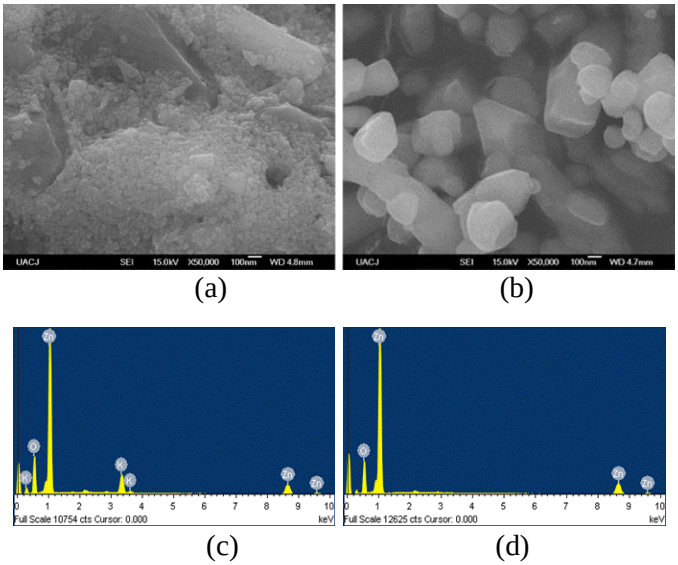

Fig. 1. Examples of SEM images of wasted alkaline battery anodes (a) and (b) and elemental chemical composition by EDS of the wasted anodes powder before (c) and after (d) washing process

The washed anodes powders were leached using nitric acid. The main reaction (reaction 1) occurring during the leaching process has been reported by [46]. For spent batteries, reactions (2) and (3) have also been reported for the Zinc dissolution but these reactions do not consider gas evolution during leaching.

$$4HNO_3 + Zn = Zn(NO_3)_2 + 2NO_2\,(gas) + 2H_2O \quad (1)$$

$$4Zn + 10HNO3 = 4Zn(NO3)2 + NH4NO3 + 3H2O \quad (2)$$

$$ZnO + 2HNO3 = Zn(NO3)2 + H2O \quad (3)$$

The thermal changes of the rice starch and dextrose dried gels were assessed by TGA analysis. (Fig. 2). In both cases, several changes occurred but three main events can be observed. The initial weight loss is 7.1% and occurs at approximately 48°C to 230°C. This corresponds to water evaporation and the chemically bond group's decomposition. The second stage is the starch dry gel weight loss (18.6%) and it is in the range from 230°C to 310°C. It has been attributed to the decomposition of organic groups [30]. Finally, the formation of a ZnO pure phase is related to the last weight loss (2.3%) that occurs in the range from 310°C to 415°C [30]. Total weight loss is 28%. When dextrose is used, the initial weight loss (6.8%) occurs in the range from 48°C to 120°C. The second weight loss (64.4%) occurs in the range of 120°C to 140°C and it is reported to occur mainly due to the hydroxyl group decomposition [47]. In this case, decomposition occurs at lower temperature than the decomposition that occurs when dried gel using starch is tested and it is due to the dextrose simpler structure. The final weight loss (in the range from 140°C to 400°C) is very subtle (1.8%) and as occur with starch is attributed to the ZnO pure phase formation.

Starch dry gel decomposition temperatures are similar to those reported by [30], except that they report a total weight loss of 52% instead the total weight loss of 28% that occurs in this case. Total weight loss for the dextrose case is 73%. Differences are significant and can be explained with the variations of initial composition. More dextrose was required as sol-gel agent because the dextrose molecule is simpler than starch. According to the reaction mechanism, proposed for these systems [30], metal cations are attracted by oxygen of the starch OH branches. A network that holds water, and increases the mixture's viscosity is formed during starch gelatinization. However, in the dextrose case, where the structure is simpler, the networking process does not easily occur and more material is required to hold the metallic cations.

Fig. 3, shows the FTIR spectra of starch and dextrose the C-O and C-C groups vibrations modes in the region of 900 to 1200 cm^{-1} and 600 to 1500 $cm^{-1}$are seen as in [30, 47]. The bands in the range from 2900 to 3450cm^{-1} are assigned to C-H and OH groups. [30,47]. Starch and dextrose dry gel show bands in the range of 1400 to 1650 cm^{-1} and 1000 to 1650 cm^{-1} which correspond to the C=O vibration modes [30]. The bands in the range 2700 and 3500 cm^{-1} are characteristic of CH and OH vibrations modes from the $Zn(OH)_2$ [30, 48]. After the calcination of both dried gels, it is observed how the characteristic band of the Zn-Oq bond appears at 440cm^{-1} and the rest of the bands disappears [30, 48].

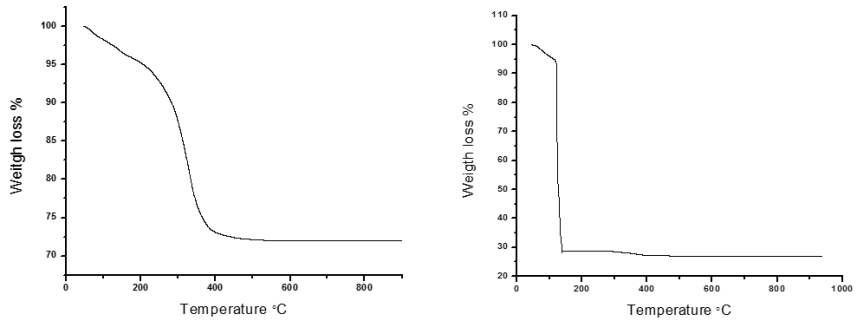

(a) (b)

Fig. 2. TGA analyses of rice starch (a) and dextrose (b) dried gels.

The diffraction patterns of the starch and dextrose samples after calcination are shown in Fig. 4. All peaks correspond to the hexagonal ZnO phase (PDF # 01-075-0576). In both cases the crystallite size increases with calcination temperature (Table 1). Crystallite size is larger when dextrose is used, except at calcinations temperatures below 600°C. This could be explained with the prompt dextrose decomposition observed in the TGA analysis. Since it decomposes faster, the thermal energy added into the system causes the crystal growth.

X-Ray fluorescence analyses were performed on anodes's powder and on synthesized nanoparticles. Only Indium traces were detected in some samples (anodes powder or nanoparticles). No other contaminants were detected. It is reported that minor amounts of additives in the range of 10 ppm to 10000 ppm, such as indium or bismuth (gassing inhibitors for reducing the undesirable tendency for hydrogen gas to build up inside the cell) are added to the anode mixture that is made of Zinc powder [49]. Indium, as element or as oxide, is classified by the NFPA as health hazard 1 which is an indicative of caution because the element may be irritating in case of eye or skin contact (e.g. CAS#: 1312-43-2, CAS#: 7440-74-6).

The differences between the synthesis with starch and dextrose can be observed in Table 1. A comparison among the crystallite calculated by Scherer's equation, particle size obtained by analysis of TEM and SEM images (Figs. 5 and 6), and Dynamic Light Scattering analysis is presented.

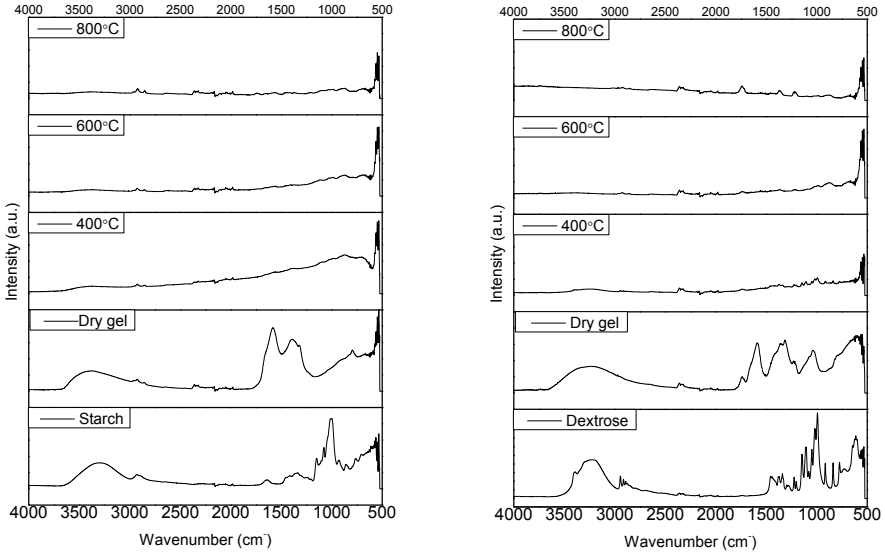

(a) (b)

Fig. 3. FTIR analyses of rice starch (a) and dextrose (b) systems

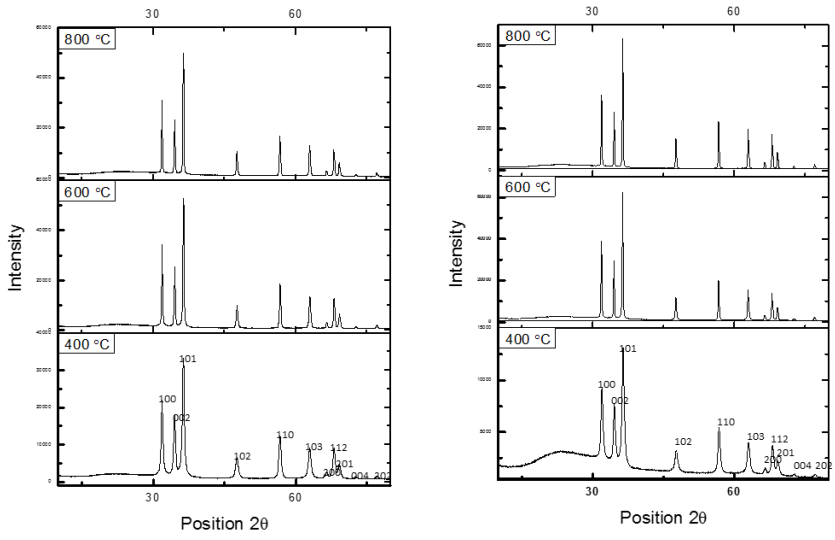

(a) (b)

Fig. 4. XRD analysis of the starch (a) and dextrose (b) samples after calcination. All peaks correspond to the hexagonal ZnO phase (PDF # 01-075-0576)

Table 1. Crystallite and particle size comparison of the ZnO NPs

Calcination Temperature °C	Crystallite size nm		SEM and TEM image analysis nm		Dynamic Light Scattering nm	
	Starch	Dextrose	Starch	Dextrose	Starch	Dextrose
400	19.3	20.3	20-32	20-29	30-45	30-42
500	31.4	29.2	43-70	48-65	32-121	30-135
600	42.2	64.8	55-85	53-93	60-145	50-171
700	52.6	70.3	60-130	82-150	63-144	72-155
800	58.5	83.6	89-160	94-165	>72	>100

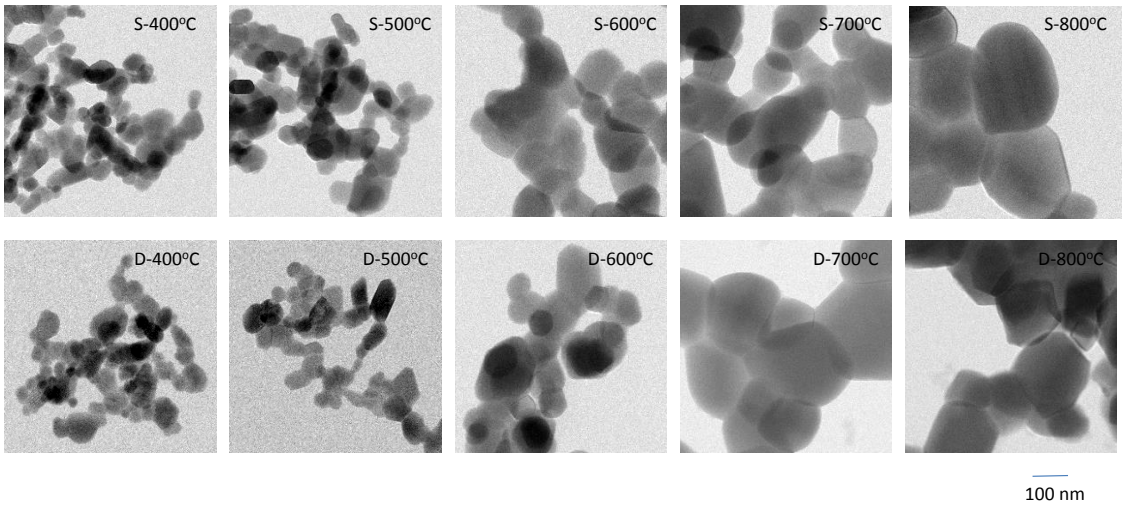

Fig. 5. TEM images showing the effect of calcinations temperatures on the size of ZnO nanoparticles synthesized using starch (S) and dextrose (D)

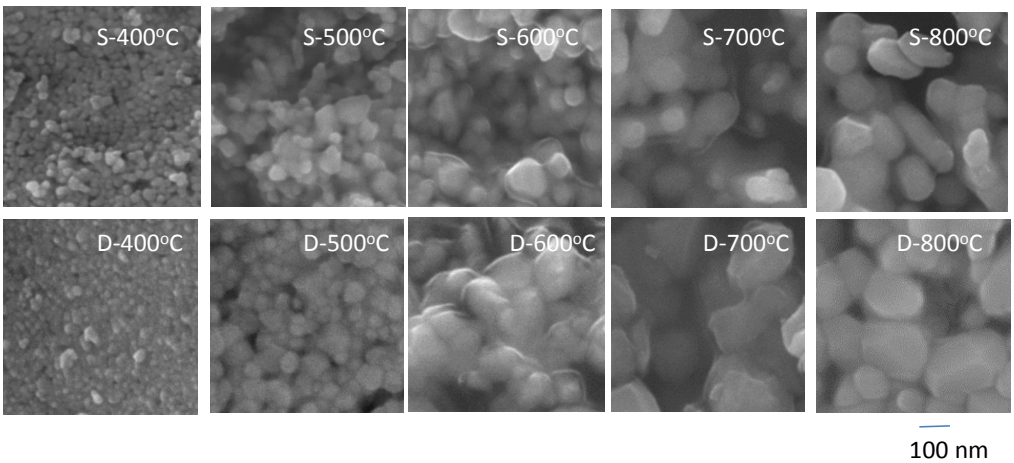

Fig. 6. FE-SEM images showing the effect of calcinations temperatures on the size of ZnO nanoparticles synthesized using starch (S) and dextrose (D)

Particles average size of the synthesis performed at 400 °C is in the range of 20 to 45 nm. When calcination is carried out at 600°C, particles in the range from approximately 50 to 100nm are mainly observed but larger particle sizes are also detected. This is because some sintering occurs between particles as can be observed in the TEM images of Figure 5. After calcination at 800°C, not only the particle size increases but also the sintering between particles increases.

Significant differences between starch and dextrose only occur at calcination temperature above 600^{o}C. Particle size is lower when rice starch is used. Dextrose is lower cost and its dry gel main weight loss occurs at lower temperatures than rice starch. Therefore, calcination time could be reduced and could allow the particle size reduction. However, the amount of rice starch required is lower than the dextrose amount which can increase the process efficiency and reduce CO/CO_2 emissions.

Fig. 7 shows the toxicity of ZnO nanoparticles in 3T3 fibroblasts cells by MTT assay for 24 and 72 h. It can be seen how the cell viability decreases when NPs concentration increases. Nevertheless, all the concentrations show cytotoxicity effect as it is showed by the percentage of viability obtained [ISO 10993-5:2009(E)].

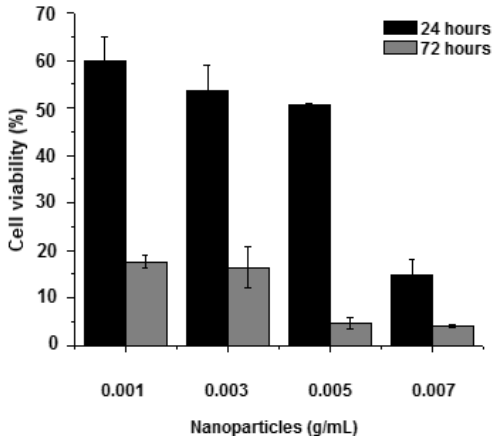

Fig. 7. MTT assay results of ZnO nanoparticles synthetized using starch and calcined at 400^{o}C

After 24 h exposure at 0.001, 0.003, 0.005, and 0.007 g/mL the percentage were 59.81, 53.57, 50.51, and 14.94 respectively decreasing at 72 h to 17.65, 16.43, 4.65, and 4.07. These results show high cytotoxicity values as reported by Brunner et al. [36]. which used same line cells, lower concentrations and similar particle size. However, other authors reported significant lower cytotoxicity (with larger or smaller particles size than this study) using same concentrations and line cells. ZnO NPs cytotoxicity is still controversial and mechanism has not been well identified [35,50]. In this case, the fact that NPs are obtained from recycled materials is likely to affect the NPs cytotoxicity since they can have impurities below the detection limits of the used characterization techniques. It is a must, for each new proposed NPs synthesis route, to determine the human hazards of the resulting NPs in order to limit their use to applications where the risk is diminished.

4. Conclusions

ZnO NPs in the range of 20 to 160 nm (depending on the calcinations temperatures) were successfully synthesized using waste alkaline batteries as zinc source. Nitric acid and starch or dextrose were used as leaching and sol gel agents, respectively. No major contaminant residues were found on the synthesized nanoparticles; only traces of Indium were found in few powder´s anodes or synthesized nanoparticles samples. The NPs in concentrations from 1 to /% showed a cytotoxic effect according ISO 10993-5:2009(E). The obtained NP´s using starch and dextrose are similar except that after 600^{o}C calcinations temperatures, that particle size is slightly smaller and more homogenous when starch is used. Nevertheless, the prompt decomposition of dextrose dried gel could allow the reduction of the calcination time and particle size.

Acknowledgments

Authors thank PRODEP and AFIPIIT from Chihuahua´s government for the support of this project as well as M.S. Carlos Ornelas of CIMAV-Mexico for his assistance with TEM images.

References

[1] D. Segets, J. Gradl, R. K. Taylor, V. Vassilev, W. Peukert, ACS Nano **3**(7), 1703 (2009).
[2] X. Lou, S. Hesheng, S. Yusheng, Journal of Transducer Technology, **3**, 1 (1991)
[3] Z. Fan, J.G. Lu, Journal of nanoscience and nanotechnology, **5**(10), 1561 (2005).
[4] D. Sharma, S. Sharma, B. S. Kaith, J. Rajput, M. Kaur, Applied Surface Science **257**(22) 9661(2011).
[5] A.P. Kumar, R.P. Shing, Bioresource Technology **99**(18), 8803(2008).
[6] J. H. Li, R. Y. Hong, M. Y. Li, H. Z. Li, Y. Zheng, J Ding, Progress in Organic Coatings, **64**(4), 504 (2009)
[7] D. Yu , R. Cai , Z. Liu Spectrochimica Acta, Part A: Molecular and Biomolecular Spectroscopy, **60**(7), 1617 (2004).
[8] R. Rajendra, C. Balakumar, H. A. M. Ahammed, S. Jayakumar, K. Vaideki, E. Rajesh, International Journal of Engineering, Science and Technology **2**(1), 202 (2010).
[9] L. Zhang, Y. Ding, M. Povey, D. York, Progress in Natural Science **18**(8), 939 (2008)
[10] X. Ma, P. R. Chang, J. Yang, J. Yu, Carbohydrate Polymers **75**(3),472 (2009),
[11] A. M. Nafchi, A. K.Alias, S. Mahmud, M. Robal, Journal of Food Engineering **113**(4), 511 (2012).
[12] D. Banerjee, J. Y. Lao, D. Z. Wang, J. Y. Huang, Z. F. Ren, D. Steeves, B. Kimball, M. Sennett, Applied Physics Letters **83**(10), 2061 (2003).
[13] Y.B. Hahn, Korean Journal of Chemical Engineering, **28**(9), 1797 (2011).
[14] T. Frade, M.E. Melo Jorge, A. Gomes, Materials Letters **82**, 13 (2012).
[15] R. Wahab, S.G. Ansari, Y.S. Kim, H.K. Seo, H.S. Shin, Applied Surface Science, **253**(18), 7622 (2007).
[16] X. Y. Kong, Y. Ding, R. Yang, Z.L. Wang, Science **303**(5662), 1348 (2004).
[17] Z. W. Pan, Z. R. Dai, Z. L. Wang, Science, **291**(5510), 1947 (2001).
[18] J. J. Wu, S. C. Liu, C. T. Wu, K. H. Chen, L. C. Chen, Applied Physics Letters, **81**(7), 1312 (2002).
[19] W.J. Chen, W.L. Liu, S.H. Hsieh, T.K. Tsai, S.Y. Chang, Applied surface science, **253**(8), 3843 (2007).
[20] J. Liu, X. Huang, J. Duan, H. Ai, P. Tu, Materials Letters, **59**(28), 3710 (2005).
[21] Y. Huang, J. He, Y. Zhang, Y. Dai, Y. Gu, S. Wang, C. Zhou, Journal of materials science, **41**(10), 3057, (2006).
[22] B. Nikoobakht, X.Wang, A. Herzing, J. Shi, Chemical Society Reviews, **42**(1), 342 (2013).
[23] L.C. Tien, S. J. Pearton, D.P. Norton, F. Ren, Journal of Materials Science, **43**(21), 6925 (2008).
[24] J. Cui, Materials Characterization, **64**, 43 (2012).
[25] B. Cheng, E.T. Samulski, Chemical Communications, **8**, 986 (2004).
[26] H.J. Zhai, W.H. Wu, F. Lu, H.S. Wang, C. Wang, Materials Chemistry and Physics, **112**(3), 1024 (2008).
[27] A.K. Zak, W.H.A. Majid, M. Darroudi, R. Yousefi, Materials Letters **65**(1), 70 (2011).
[28] H. Staroszczyk, P. Janas, Carbohydrate Polymers, **80**(3), 962 (2010).
[29] G. Zhang, X. Shen, Y. Yang, The Journal of Physical Chemistry C, **115**(15), 7145, (2011).
[30] A. Khorsand Zak, W.H. Abd. Majid, M.R. Mahmoudian, M. Darroudi, R. Yousefi, Advanced Powder Technology, **24**(3), 618 (2013).
[31] M. N. Nadagouda, R. S. Varma, Smart materials and structures, **15**(5), 1260 (2006).
[32] S. Mukherjj, Saha, M. ““Route Sol-Gel. "Synthesis of Copper-Silica, Cobalt-Silica & Nickel-Silica Nanocomposites."”” PhD diss., Jadavpur University, 2012.

[33] V. Sharma, R. K. Shukla, N. Saxena, D. Parmar, M. Das, A. Dhawan, Toxicology letters, **185**(3), 211 (2009).
[34] H.J. Wang, Y.Y. Sun, Y. Cao, X.H. Yu, X.M. Ji, L. Yang, Chemical Engineering Journal, **178**, 8 (2011)
[35] Y. Zhang, K. C. Nguyen, D.E. Lefebvre, P. S. Shwed, J. Crosthwait, G. S. Bondy, A. F. Tayabali, Journal of Nanoparticle Research, **16**(6), 2440 (2014)
[36] T. J. Brunner, P. Wick, P. Manser, P. Spohn, R. N. Grass, L. K. Limbach, A. Bruinink, W. J. Stark, Environmental Science and Technology, **40**(14), 4374 (2006)
[37] A. Sirelkhatim, S. Mahmud, A. Seeni, N. H. M. Kaus, L. C. Ann, S. K. M. Bakhori, H. Hasan, D. Mohamad. Nano-Micro Letters, **7**(3), 219 (2015)
[38] N. Lewinski, V. Colvin, R. Drezek. Small, **4**, 26 (2008)
[39] J.I. Tariq Jan, M. Ismail, M. Zakaullah, S.H. Naqvi, N. Badshah, International Journal of Nanomedicine, **8**, 3679 (2013)
[40] J.J. Wang, J.S.B. Sanderson, H. Wang, Mutation Research, **628**(2), 99 (2007)
[41] N. M. Franklin, N. J. Rogers, S. C. Apte, G. E. Batley, G. E. Gadd, P. S. Casey, Environmental Science & Technology, **41**(24), 8484 (2007)
[42] A. Tkachenko, H. Xie, D. Coleman, W. Glomm, J. Ryan, M. Anderson, S. Franzen, D. Feldheim, Journal of the American Chemical Society, **125**(16), 4700 (2003)
[43] M. Berger, Nanotechnology could make battery recycling economically attractive, NanoWerk, http: http://www.nanowerk.com/spotlight/spotid=23592.php (2011).
[44] G. Belardi, P. Ballirano, M. Ferrini, R. Lavecchiac, F. Medici, L. Pigac, A. Scoppettuoloc, Thermochimica Acta **526**(1-2), 169 (2011)
[45] S.M. Xara, J.N. Delgado, M.F. Almeida, C.A. Costa, Waste Managment, **29**(7), 2121 (2009)
[46] P. Hu, D. Pan, S. Zhang, J. Tian, A.A. Volinsky, Journal of Alloys and Compounds, **509**(9), 3991 (2011)
[47] M. Ibrahim, M. Alaam, H. El-Haes, A. F. Jalbout, A. de Leon, Eclectica Quimica **31**(3), 15 (2006)
[48] C. Pholnak, C. Sirisathitkul, S. Suwanboon, D. J. Harding, Materials Research, **17**(2) (2014)
[49] R. E. Durkot, L. Lin, P. B. Harris, ZINC ELECTRODE PARTICLE FORM, Duracell Inc., Bethel, CT (US), Patent No. US 6, 284, 410 B1 (2001).
[50] F. Namvar, H. S. Rahman, R. Mohamad, S. Azizi, P. M. Tahir, M. Stanley Chartrand, S. K. Yeap, Evidence-Based Complementary and Alternative Medicine, **2015**, 1 (2015)